Inundation and Potentials Hazard Analysis of Landslide Lake

Attaabad-Hunza, Pakistan

By

HAFSA FIRDOUS

A thesis submitted in partial fulfillment of the requirements for the degree of Master of Science in Remote Sensing and GIS

Institute of Geographical Information Systems
School of Civil and Environmental Engineering
National University of Sciences & Technology
Islamabad, Pakistan

August 2012

CERTIFICATE

Certified that content and form of thesis entitled "**Inundation and Potential Hazard Analysis of Landslide Lake Attaabad-Hunza, Pakistan**" submitted by Ms. Hafsa Firdous has been found satisfactory for the requirements of Master of Science degree in Geographic Information Systems and Remote Sensing.

Supervisor: _____

Dr. Javed Iqbal,
Associate Professor & HoD
IGIS-NUST, Islamabad

Member: _____

Eng. Sarwar Jamal
Associate Dean, IGIS-NUST, Islamabad

Member: _____

Col Sarfraz Ali
Associate Professor, MCE, NUST, Risalpur

Member: _____

Mr. Saad Saleem Bhatti
Lecturer, IGIS, NUST, Islamabad

External Examiner:

Signature _____

Name_____

Designation_____

ACADEMIC THESIS: DECLARATION OF AUTHORSHIP

I, Hafsa Firdous, declare that this thesis and the work presented in it are my own and have been generated by me as the result of my own original research.

Inundation and Potential Hazard Analysis of Landslide Lake Attaabad-Hunza, Pakistan.

I confirm that:

1. This work was done wholly by me in candidature for an MS research degree at the National University of Sciences and Technology, Islamabad.
2. Wherever I have consulted the published work of others, it has been clearly attributed.
3. Wherever I have quoted from the work of others, the source has been always cited. With the exception of such quotations, this thesis is entirely my own.
4. I have acknowledged all main sources of help.
5. Where the work of thesis is based on work done by myself jointly with others, I have made clear exactly what was done by others and what I have contributed myself.
6. None of this work has been published before submission. This work is not plagiarized under the HEC plagiarism policy.

Signed: ……

Date: ……

DEDICATION

To

My Sweet & Loving Parents

ACKNOWLEDGEMENTS

First of all, I will like to thank Allah Almighty, the most Gracious and Merciful.

My warm gratitude and unfathomable appreciation go to tremendously patient, very friendly and extremely supportive attitude of my respected research Supervisor Dr. Javed Iqbal, who always helped me whenever the need arose. His precious advices always proved prolific for me. I have always enjoyed and erudite from engaging in stimulating and energizing discussions with him.

If not for the considerate insight and capabilities of my committee members, Eng. Sarwar Jamal, Col. Sarfraz Ali and Mr. Saad Saleem this thesis would conceivably not have seen the light of day. They not only extended their full support but also facilitate me in refining and completing this work under their intellectual guidance.

I would like to extend my sincere appreciation to NESPAK Lahore, Pakistan, WAPDA, Lahore, Meteorological Department and Soil Survey of Pakistan, Peshawar for providing me with all the essential data for this research.

Lastly, I has no words to express gratefulness to my family and friends who always pray for my success, triumph and support me in every walk of life.

Hafsa Firdous

Table of Contents

LIST OF FIGURES

LIST OF TABLES

LIST OF NOTATIONS

Notation	Explanation
et al.	“and the rest”
#	Number
°	Degree
’	Minutes
etc.,	et cetera
∂	Partial Differential
E.g.	Example
MCM	Million Cubic Meter
%	Percentage

LIST OF ABBREVIATIONS

Abbreviation	Explanation
ASTER	Advanced Space borne Thermal Emission and Reflection Radiometer
DEM	Digital Elevation Model
ETM	Enhanced Thematic Mapper
EROS	Earth Resources Observation & Science Center
ERDAS	Earth Resources Data Analysis Systems
GIS	Geographical Information Systems
GUI	Graphical User Interface
HEC	Hydrological Engineering Center
HEC-RAS	Hydrological Engineering Center River Analysis System
HEC-GeoRAS	Hydrological Engineering Center Geospatial River Analysis System
LLOF	Landslide Lake Outburst Flood
NASA	National Aeronautics and Space Administration
USGS	United States Geological Survey

ABSTRACT

The landslides considered to be very perilous among the natural hazards and it become more destructive if it blocks the flow of river creating a landslide lake. On 4th January, 2010 landslide occurred close to the Attaabad village approximately 80 km upstream from Gilgit. The landslide blocked the flow of Hunza River and created Landslide Lake. The landslide occurred at the fault line and created highly crushed rock mass. The objectives of the study were to model and simulate Landslide Lake Dame break and map the potential area at risk downstream due to the flood inundation in case of dam breach. To achieve the objectives of the study a joint approach of GIS, remote sensing and hydrological modeling was used for flood simulation. Hydrologic Engineering Center's River Analysis System (HEC - RAS) with its GIS embedded extension HEC-GeoRAS was used. The data used include ASTER 30-m digital elevation model (DEM), peak flow discharge at landslide location, land use map (Manning's *n* values) and satellite imageries. HEC-GeoRAS was used to develop the RAS layers geometry including River Centerline, banks, flowpaths, inline structure and cross-sections from Triangulated Irregular Network (TIN). The data was then used as an input to HEC-RAS for unsteady flow simulation. Data input in the model include recoded monthly flow average, normal water depth, and inline structure breach parameters. The HEC-RAS generated water surface profile, velocity and flow hydrographs. The results of the HEC-RAS were finally mapped in ArcGIS for flood extent, flood water depth and flood wave velocity. The water depth, velocity and time to reach maximum discharge were calculated for all the inundated villages. The result of the study indicated that out of 26 villages 7, 10, and 9 villages were classified as at high, medium and low risk, respectively. This approach could be used for development of early warning and emergency preparedness plans to save the livelihood and property.

Chapter 1

INTRODUCTION

The movement of a mass of rock or soil down a slope is known as landslide. It occurs when the force of gravity deploying on the materials on an inclined surface overwhelms the material's resistance to shearing. If this mass of rock or soil blocks the flow of river over long period, than it creates artificial lake known as Landslide Lake.

1.1 Landslide Lake History

The history of landslide-dammed rivers is very old. In 1737 BC the literature about landslide dammed rivers was documented in Hunan Province in central China, when Lo and Yi rivers were dammed due to an earthquake triggered landslide (Xue-Cai and An-ning, 1986). The literature about afterward consequences of landslide dammed rivers i.e. Landslide Lake Outburst Flood (LLOF) was documented, in 563 AD in Switzerland (Eisbacher and Clague, 1984) and also in 1006 AD in central Java (Holmes 1965). In 1786 the world's most perilous LLOF was recorded in Sichuan Province, China. The Kangding Louding earthquake activated a massive landslide and blocked the Dadu River creating Landslide Lake, which was overtopped and busted after 10 days resulting in a LLOF affecting about 1,400 km downstream and drowned about 100,000 people (Schuster 2000). In 1911 world massive and deepest (550–700 m) historic landslide lake was created in Tajikistan due to earthquake that activated a 2–2.5 billon m^3 landslide and blocked the Murgab River (Gasiev, 1984; Schuster, 2000). In recent events of LLOFs due to busting of landslide lakes in the Tibetan region of China in the Trans-Himalayan region along Paree Chu (stream) and the Satluj River were documented during 2000 and 2005 respectively. It affects the waterway and communications & Transportation in Himachal

Pradesh province, India in the Kinnaur district. It has been studied that the loss of property and life due to these LLOFs is directly proportional to the characteristics of the materials. (Gupta and Sah, 2008)

Landslides can occur due to physical, morphological, geological and human induced causes. Some of causes are given in the table 1.1.

1.2 Global Studies on Landslide Lakes

Cui, Zhu, Han, Chen and Zhuang in 2009 studied, the distribution and preliminary risk of landslide lakes formed due to 12 May Wenchuan earthquake in China. Landslides and rock avalanches produced 257 landslide lakes. The authors traveled to the landslide prone area to observe some of the physical properties of the debris dams. Their work summerises about the characteristics of the Wenchuan earthquake landslide lakes together with their classification and distribution. The lakes were classified as extremely high risk, medium risk, and low risk according to field observations and remote sensing. They evaluated the dam breach risks for 21 debris dams. They also analyzed the trend toward the future occurrences of earthquake triggered landslide lakes in the years following for hazard mitigation. (Cui, Zhu, Han, Chen & Zhuang, 2009)

On 21 September 1999 massive landslides induced by the Chi-Chi earthquake (ML = 7.3) blocked up gorges of Ching-Shui creek, and produced landslide lake. Although emergency spillways was constructed to prevent dam failures, but there was a threat of overtopping and breaching due to excessive inflows in raining seasons. This research work was conducted to simulate and to analyze the inundation potentials downstream of Tsao-Ling Landslide Lake using a hydrologic/hydraulic approach and

Table 1.1. Geological, morphological, physical and human causes for landslides.

Geological causes	**Morphological causes**	**Physical causes**	**Human causes**
Rainfall and snow fall Weak materials Sensitive materials Sheared materials Weathered materials Fissured materials Adversely orientated discontinuities Material contrasts Permeability contrasts	Uplift Rebound Slope angle Wave erosion Fluvial erosion Glacial erosion Subterranean erosion Erosion of lateral margins Vegetation change Slope loading	Rapid snow melt Intense rainfall Prolonged precipitation Earthquake Volcanic eruption Seismic activity Thawing Freeze-thaw Rapid drawdown Ground water changes Soil pore water pressure Surface runoff	Loading Excavation Drawdown Mining Land use change Water management Water leakage Vibration Quarrying Yodeling Deforestation

GIS (Geographic Information System) technology. Hydrologic analysis was used to illustrate regional rainfall-runoff characteristics and to design rainfall/runoff scenarios. One-dimensional dam break flood routings were performed using the DAMBRK model of NWS (National Weather Service, USA) with different return periods (20, 100 and 200years) of rainfall events and dam failure durations for downstream creeks. The depletion hydrographs of dam break routings were applied into two-dimensional overland flow simulations using FLO-2D model for downstream lowlands. The results of hydraulic computations were evaluated with GIS maps for inundation potentials analysis, which could be used to assist the planning of emergency response measures. (Li, Hsu, Hsieh & Teng, 2002).

1.3 HEC-RAS

Hydrologic Engineering Center's River Analysis System (HEC - RAS) is an embedded system and software, which is developed for a multi-tasking and multi-user network in interactive environment. HEC - RAS is consisted of a graphical user interface (GUI), separate hydraulic analysis components, graphics and reporting facilities, data storage and management capabilities. The system contains three one-dimension hydraulic analysis components for:

Steady flow water surface profile components, unsteady flow water surface modeling and variable boundary sediment transfer calculations (Brunner, 2010).

1.3.1 Steady Flow Water Surface Profile

HEC-RAS is proficient to execute 1 - D water surface profile computation for steady progressively hanging flow in constructed or natural water channels. Subcritical, supercritical, and mixed flow system water surface profiles can be computed (Brunner, 2010).

Water surface profiles are calculated from one cross section to the next. It is done by the standard step method in which energy equation is solved with iteration method. The Energy equation is given below.

$$Y2 + Z2 + \alpha 2V22/2g = Y1 + Z1 + \alpha 1\, V12\, /2g + he \quad \text{..... (1)}$$

Where:
Y1, Y2 = water depth at cross sections
Z1, Z2 = elevation of the main channel inverts
V1, V2 = average velocities (total discharge/ total flow area)
α1, α2 = coefficients of velocity weighting
g = acceleration due to gravitational
he = energy head loss

1.3.2 Unsteady Open Channel Flow

The unsteady flow simulation is done in HEC-RAS model by solving the full 1 D St Venant equation for unsteady open Channel flow.

$$Qc = \Phi Q \quad \text{..... (2)}$$

$$\partial A/\partial t + \partial \Phi Q/\partial xc + \partial(1 - \partial\Phi)Q/\partial Xf = 0 \quad \text{..... (3)}$$

$$\partial Q/\partial t + \partial(\Phi 2Q2/Ac)/\partial xc + \partial/\partial Xf\,((1 - \Phi 2)Q2/Af)gAc\,(\partial Z/\partial Xc + Sc) + gAf\,(\partial Z/\partial Xfa + Sf) = 0 \quad \text{..... (4)}$$

Where:
Qc = channel flow,
Q = total flow
Φ = Kc / (Kc+Kf)
Kc = transportation in the channel
Kf = transportation in the floodplain
A (Ac, Af) = cross-section area of the flow (in Channel, floodplain),
Xc , Xf = Distances along the channel and floodplain
P = wetted perimeter
R = Hydraulic radius
n= Manning's roughness Value
S= Friction Slope
Φ = flow partitioned between the channel and floodplain

1.4 Attaabad Landslide Lake

Attaabad is located about 10km upstream of Karimabad, high up on west side of valley, just beyond the great mid 19th century (1858) mud-flow dam across the Hunza

river gorge. This was an unusual event creating a temporary blockage about 300m high. Remnants of the dam following its failure are still to be seen today, forming a significant topographic feature.

Sometime during the first week of February 2003 a 'crack' was noticed in the ground above Attaabad village (Hunza valley, Northern Areas Pakistan). The crack was map out uphill all the way through steep scree slopes and it became gradually bigger until reaching the peak rock facade and then swung back downhill until intersecting with the Hunza ravine cliff edge. Following inspection of the situation, by members of the Aga Khan Regional Council for Hunza and FOCUS (a Pakistan NGO for disaster preparedness), it was planned to evacuate many people living down slope of on the cracked part of the mountain. It gave all the signs of being initializing a large landslide. It was estimated that cracking is caused by a destructive earthquake (ML = 6.5), that was occurred on 16th November 2002 (E 74°.45" N35°.30") at the junction of the Astor Valley with the Indus Valley. The earthquake was followed by many considerable foreshocks and many major aftershocks that continued for quite a lot of months (Hughes, EEFIT).

On January 4, 2010 a massive landslide close to Atta Abad village occurred, with a 450 feet-high mud-and-stone wall blocking the flow of the Hunza River and creating an artificial lake. The lake is now at least 15 kilometres long and one-and-a-half kilometre wide, stretching from Hussaini village to Atta Abad. Five villages, Ainabad, Shushkut, Gilmat, Attaabad, Phasoo and Hussaini, have already been flooded and another three villages were in danger of being inundated by the artificial lake. The landslide also flounced away a major section of Karakoram Highway that links China with Pakistan. Chinese and Frontier Works Organization (FWO) engineers instigated cutting the 196,000 m^3 high debris down to 30 m (Mir, 2010).

The main objectives of the study were (i) Landslide debris composition analysis, (ii) Hydraulic computation with GIS embedded for inundation potential analysis in case of landslide lake outburst scenario. The sub-objectives of this part were preparation of classified maps showing the potential inundation areas, flood routing and flood levels and flood velocities mapping.

Chapter 2

MATERIALS AND METHODS

2.1 Study Area

The study area situated between 74° 47’ 18” E – 74 ° 52’ 20” E and 36 ° 20’ 56” N – 36 ° 17’ 29” N. The area is about 760 km from the Islamabad and 30 km from the Aliabad, the main town of Hunza valley (figure 2.1). It is bounded by the villages Attaabad and Gulmit on west and east bank of the river Hunza, respectively and Karakoram highway on east of the river.

Attaabad is an old conventional village of 80 families, with half the population allied to the inhabitants of Ganish and partly to Karimabad. Attaabad village is situated in a rough grazing land environment, being small and bounded by natural slopes with meager vegetation. The local Attaabad peak to the north is at 5184m and this go up to the northwest up to Ultar Peak at 7388m. Typically, there is 150mm to 0.30m of snow and very little rain at any time in the year (Hughes, EEFIT).

2.2 Datasets Used

2.2.1 Topographic Map

Topographic sheets of scale 1: 25,000 were acquired from Survey of Pakistan (SOP) for the study area. It was used for the preparation HEC-RAS input datasets (river banks, river center line and for flow paths).

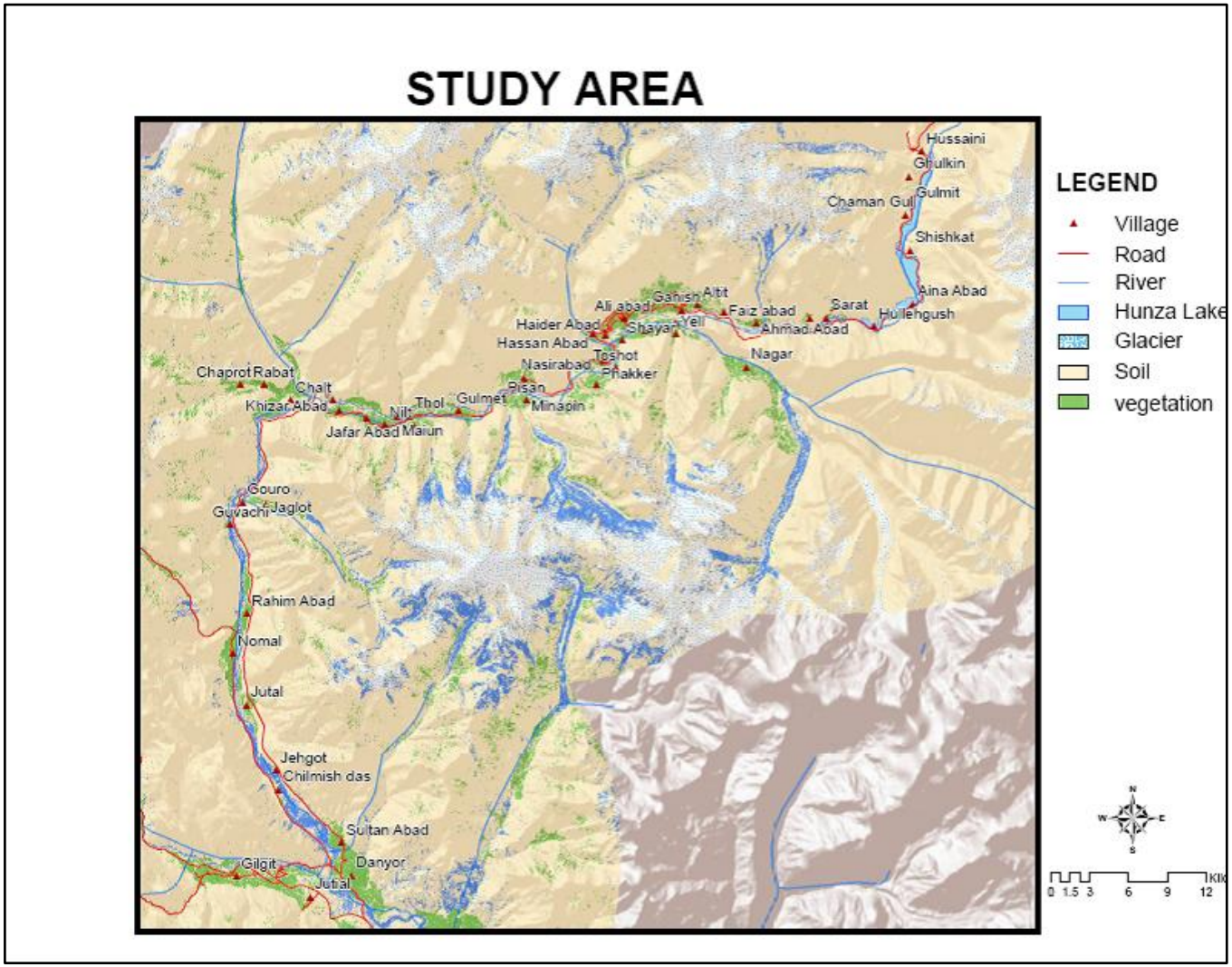

Figure 2.1. Map showing the study area.

2.2.2 Satellite Imagery

LANDSAT-7 ETM+ multispectral images with 30m and panchromatic with 15 m ground resolution were downloaded from U.S. Geological Survey, Earth Resources Observation & Science Center (EROS) website (table 2.1 & 2.2 Appendix – 1). The imagery acquisition date was 19th June, 2010. Study area was fall in two images which were mosaic and preprocessed. After extracting the study area the image was used to prepare land use/land cover map.

2.2.3 Digital Elevation Model

Digital elevation model (DEM) of 30m produced by Shuttle Radar Topography Mission (SRTM) was downloaded from United States Geological Survey (USGS) website. DEM was used to generate triangular irregular network (TIN) (Appendix – 2).

2.3 Field Visit

A field visit to study area was conducted during the last week of June, 2010. The aims of the field visit were to collect soil and rock sample, visual observations of landslide lake and debris material and conducting interviews of the local community and lake monitoring authority. The soil (debris) samples were analyzed in laboratory for its mineralogical composition analysis.

Table 2.1. Spectral, radiometric and temporal resolution of LandSat 7 ETM+.

SPATIAL	**SPECTRAL**	**RADIOMETRIC**	**TEMPORAL (Revisit Period)**
15 m	Pan Chromatic (Single Band)	8 Bit	16 Days
30 m (Band 1-5 & 7); 60 m (Band 6)	Multi Spectral (7 Bands)	8 Bit	16 Days

Table 2.2. Spectral and spatial resolution of LandSat ETM+ bands.

Band Number	**Band Type**	**Spectral Resolution (µm)**	**Spatial Resolution(m)**
1	Blue	0.45 - 0.515	30
2	Green	0.525 - 0.605	30
3	Red	0.63 - 0.690	30
4	NIR	0.75 - 0.90	30
5	SWIR	1.55 - 1.75	30
6	TIR	10.40 - 12.5	60
7	SWIR	2.09 - 2.35	30
Pan	Pan Chromatic	0.52 - 0.90	15

2.3.1 Laboratory Tests

The soil (debris) samples were tested in laboratory for physical properties which includes soil texture, grain size, degree of saturation and porosity.

2.3.2 Sieve Analysis

Sieve analysis (or gradation test) is a method utilized to evaluate the particle size distribution (also known as gradation) of any grainy material. Sieve analysis can be conducted on all granular non-organic or organic materials as well as on crushed rock, sands, clays, granite, feldspars, coal and soil up to a smallest size depending on the exact procedure (Reddy, UIC).

The collected samples were passed through the sieve opening 19.1mm, 12.5mm, 9.5mm, 4.75mm, 2.0mm, 0.43mm, 0.15mm, 0.075mm. The weight retained and cumulative retained weight in gm was measured and percentage passing of each sample was recorded.

2.3.3 Atterberg's Limit Test

The Atterberg's limits are fundamental evaluators of the characteristics of fine grained soil. Taking in view the water amount of the soil, it can appear in four states: solid, semi-solid, plastic and liquid (figure 2.2). In each state the behavior and consistency of soil sample is different. Therefore, one can define the limit between each state depending on how soil's behavior changes. The Atterberg limits methods can be utilized to discriminate between clay and silt, and it can differentiate between different kinds of clay and silts. These limits were defined by a Swedish chemist Albert Atterberg, and later refined by Arthur Casagrande. In this study the Atterberg's limits was used to evaluate liquid limit and plastic limit (Geotechnical Engineering Bureau, 2007).

Plastic limit is the depiction of soil behavior in its shear strength while water amount rises. The water content defines where the soil alters from a semi-solid to a plastic (flexible) state. The weight of wet soil + container, weight of dry soil + container, weight of water, weight of container, weight of dry soil and water content was measured and noted down. The plastic limit of the samples was found out by rolling out threads of fine sample of soil on a non-porous flat surface that was a glass slab. The threads were rolled out for each sample (Geotechnical Engineering Bureau, 2007). Liquid limit is the amount of water at which soil alters it behavior from plastic state to liquid viscous fluid state. A part of soil sample was mixed with water in a rounded bottomed porcelain bowl. A channel was cut through the part of soil sample with a spatula. The bowl was then hit several times beside the palm of one hand. Casagrande apparatus and procedure was used to take repeatable measurements. Soil sample was put into a metal cup and a channel was cut down in middle with a tool of 13.5mm (0.53 in) width. The metal cup was then dropped on a tough rubber base at a frequency of 120 blows per minute. Due to blows impact the channel closed up gradually. The number of blows for the channel to make close was determined and recorded. The number of blows to close down the channel for different water content, container weight, weight of wet soil + container, weight of dry soil + container, weight of water, weight of dry soil was measured. The water content at which it takes 25 blows of the cup to make the channel to close for a distance of 13.5 mm is known as the liquid limit. The test was performed for several water contents. The water content at which 25 blows were required to close the channel was determined from the test results (Geotechnical Engineering Bureau, 2007).

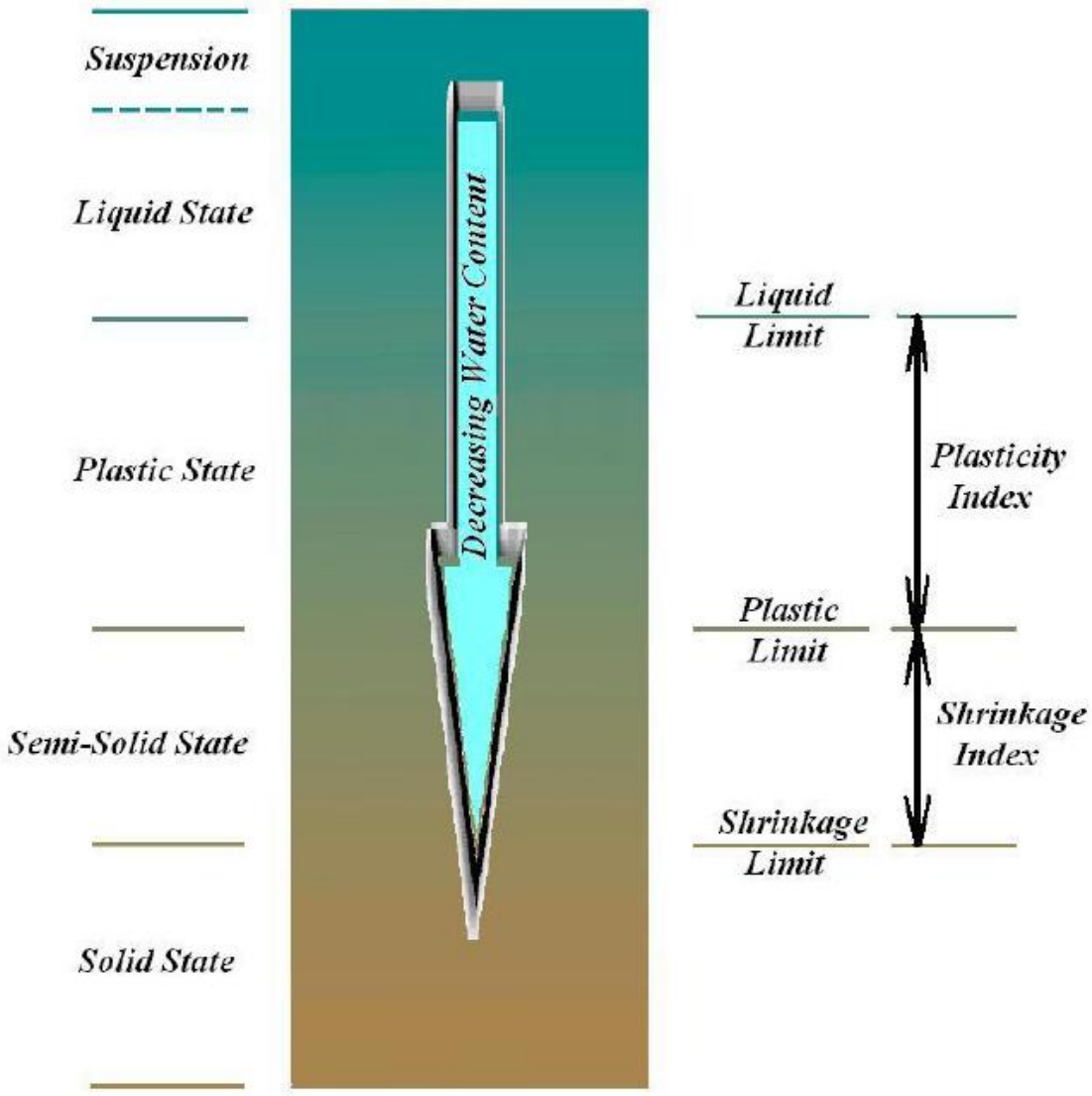

Figure 2.2. Liquid, plastic and shrinkage limits of soil (Geotechnical Engineering Bureau, 2007).

2.3.4 Plasticity index

Plasticity index (P.I) is defined as the computation of the plasticity of a given soil sample (UTA, 2004). Soil with high P.I have a tendency to be clay, with lower P.I have a tendency to be silt and with P.I = 0 are non plastic or little or no silt and clay. P.I and its ranges are given below.

0 - Nonplastic

(1-5)- Slightly plastic

(5-10) - Low plasticity

(10-20)- Medium plasticity

(20-40)- High plasticity

>40 Very high plasticity

The plasticity index was measured using following equation:

$$P.I = L.L - P.L \quad \text{..... (5)}$$

Where:
P.I = Plasticity index
L.L = Liquid limit
P.L = Plastic limit

The soil was then classified according to the Unified Soil Classification system (GREE).

2.4 Data Preparation and Methodology

All the dataset was prepared in ArcGIS 9.2 using the HEC-GeoRAS extension and ERDAS IMAGINE9.2 (figure 2.3).

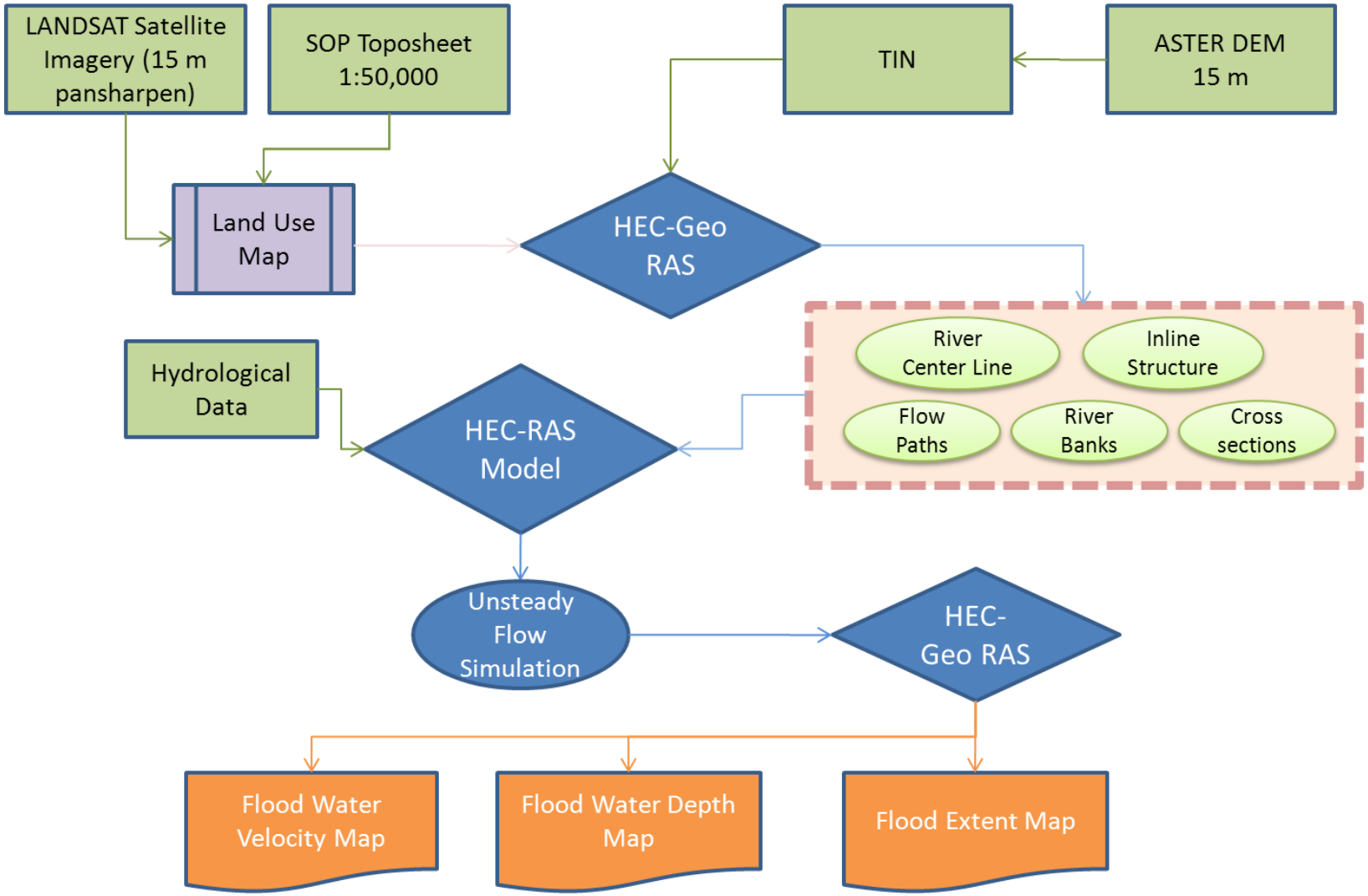

Figure 2.3. Methodology flow chart.

2.4.1 River Geometry

River geometry was created in ArcGIS 9.2 using the HEC-GeoRAS extension. HEC-GeoRAS uses separate data frames for pre and post processing of data. Projected coordinate system was applied to data frame as it is ought to have same coordinate system for all datasets and data frames. River banks were used to differentiate the main channel from the overbank floodplain areas. Information related to bank locality is used to allocate different properties for river cross-sections. The left bank was digitized first followed by the right bank while looking in downstream direction. The river center line is used to set up the river reach network for HEC-RAS. The Hunza River center line was digitize in the direction from upstream to downstream, while considering the approximate river center points. After digitizing the attributes were assigned to the center line. In HEC-RAS the flow path lines are used to calculate the downstream reach lengths between the cross-section in main channel and overbank areas. The flow path lines are of three types: centerline, left overbank and right overbank. The river center line which was created earlier considered as center flow path line. The left flow path was digitized first followed by the right overbank from upstream to downstream direction within the floodplain area. After digitization the attributes were assigned to the flow path lines as channel, left and right.

Cross-sections are very important and key input to HEC-RAS. Cross-section cutlines are used to extract the elevation data from train (TIN) to create ground profile across channel flow. The meeting point of cutlines with other RAS layers for instance centerline and flow path lines are used to calculate HEC-RAS attributes such as bank stations (locations that separate main channel from the floodplain), downstream reach lengths (distance between cross-sections) and Mannings *n* value (Merwade, 2009). Following guidelines were considered while digitizing the cross-sections cutlines: 1) they were

digitized perpendicular to direction of flow; 2) they were span over entire flood extent to be modeled; 3) and they were digitized from left to right while looking in downstream direction. Also consisting spacing between the cross-sections were maintained. After digitization the next step was to assign attributes to the cross-sections cutlines. River and reach name was copied to cutlines. Next station numbers (distance from each cross-section to the downstream end of the river) were assigned. Finally the distances to next downstream cross-section for all cutlines were calculated on the bases of flow paths. The cross-sections were still in 2D with no elevation information. These were converted into 3D on the basis of TIN.

The landslide debris material was considered as inline structure. It was digitize from left overbank to right overbank. After digitization the top width and distance to next upstream cross-section in the inline structure attributes was entered in the attribute table of the inline structure.

2.4.2 Land Use / Land Cover Map

The information of land cover/land use is significant for many planning and management activities as it is considered as an important component for modeling and understanding the earth features. The word land use relates to the human activity or economic utility associated with a particular portion of earth, while the word land cover relates to the nature of features present on the surface of the earth (Lillesand and Kiefer, 2000).

The satellite image was used to extract the up to date information of land use land cover. This land use and land cover information was later used to assign the surface roughness values i.e. Manning *n* values to river cross-sections. Landsat-7 seven band multispectral images with 30 m and panchromatic 15 m spatial resolution were used. The

images were imported to ERDAS IMAGINE software compatible format (.img), mosaicked and extracted for the study area.

The supervised classification method was used for image classification. The different band combinations were used to collect signature of different land features. The field survey information/knowledge was also used to identify the different land surface features. The signatures were collected on the basis of maximum likelihood method and defining the feature space signatures. The image was classified in different class which are: water, glaciers, bare soil, rock land, urban and vegetation for the study area (figure 2.4).

The contingency matrix was used to evaluate and asses the accuracy of the signatures that were created using the AOI in image. This matrix of percentages was used to evaluate the numbers of pixels in each AOI training samples assigned to each class.

2.4.3 Assigning the Manning's *n* Value

The last task before exporting the GIS data to HEC-RAS geometry file is assigning Manning's *n* value to individual cross-sections cutlines (Merwade, 2009). The classified land use/land cover raster map was converted into vector date shape file. These manning's *n* values were assessed on the basis of research literature (ODOT, 2010). Later these values were entered in the attribute table for different land use/land cover classes. The next step was to assign these manning's *n* values to river cross-sections. Depending on the intersection of cross-sections with land use/land cover polygons, manning's values were extracted for each cross-section.

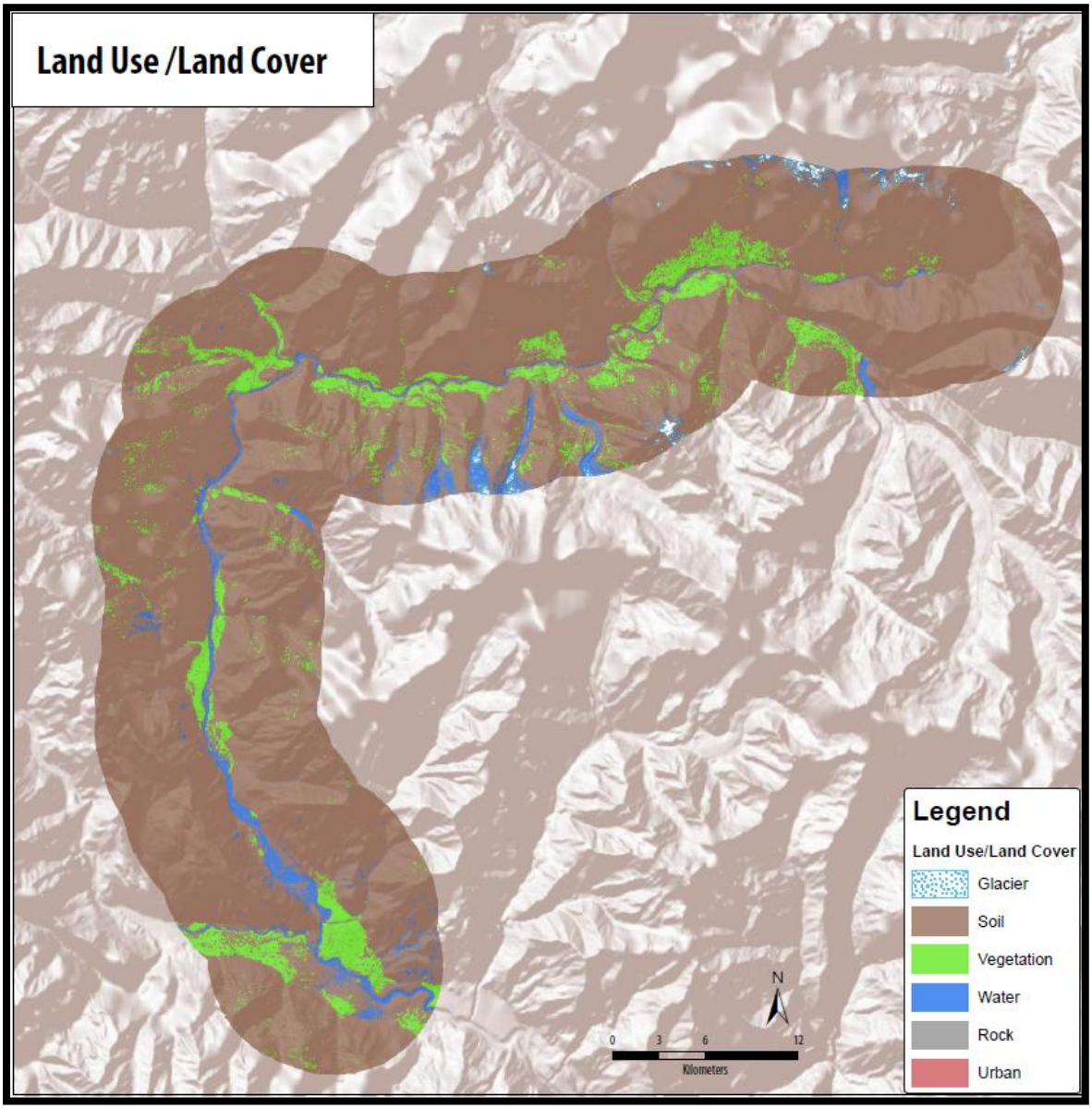

Figure 2.4. Land use/ land cover map.

2.4.4 HEC-RAS Model Execution

The GIS river geometry files were exported to HEC-RAS compatible files before executing the HEC-RAS. In HEC-RAS these files were imported and quality check was performed to ensure no erroneous data was imported from GIS. The unsteady flow data was entered using the unsteady flow data editor window. The boundary conditions for Hunza River main reach were entered. The flow hydrograph was entered for the upstream as the estimated monthly flow at the landslide location was provided. Next the initial flow data was entered using the initial condition tab in unsteady flow data editor. The initial flow was assumed 3,319, 578 ft^3/s.

After entering all the necessary input information for unsteady flow analysis in the model, the HEC-RAS model was executed for unsteady flow analysis. Computation interval was set to 20 minutes. As it should be small or a rule of thumb is to use a computational interval which is equal to or less than the time of rise of hydrograph divided by 20. The hydrograph output interval was set to 1 hour and detailed output interval was set to 2 hours. Finally, the unsteady flow was computed. After computing unsteady flow analysis the output files of flood inundation extent and flood velocities were exported to GIS format.

2.4.5 Flood Inundation Mapping in ArcGIS

The results of HEC-RAS were imported to ArcGIS using the HEC-GeoRAS extension. The flood inundation extent and water depth maps were prepared and analyzed. Moreover, flood velocities map was generated.

Chapter 3

RESULTS AND DISCUSSIONS

This research study evaluate the potential inundation and hazard analysis of Landslide Lake and the composition of landslide debris material. Initially the visit to the study area was conducted and soil and rock samples were collected. Later those samples were tested in laboratory for their composition analysis. The inundation and flood extent simulations were performed in HEC-RAS and later the resulted maps were produced in ArcGIS. This section will discuss the detail analysis of laboratory test and resulted maps and graphs.

3.1 Debris Physical Properties and Composition Analysis

3.1.1 Sieve Analysis Results

Three different soil samples were test in laboratory for the composition and texture analysis. The dry weight of the samples was 500gms. The percentage passing of sample no. 1 was 97.5% from sieve # 200. On the bases of percentage passed it was analyzed that 0% gravel was present in the sample, the sand was 2.5% and silt and clay was 97.5%. Hence the sample was classified as clay according to Unified Classification system. The percentage passing of sample no. 2 from sieve # 200 was 96.8%. On the basis of percentage passing it was evaluated that the 0% gravel, 3.2 % sand and 96.8% silt and clay was present in the sample. This sample was also classified on the basis of Unified Classification System as clay. The percentage passing of sample no. 3 was only 5.2% but from sieve opening 1/2" was 100%. According to the percentage passing through different sieves it was observed that 37.8% gravel, 57.05% sand and only 5.2% silt and clay was present in the sample.

After testing all the samples average was computed. The results evaluate that 12.7% gravel, 20.7% sand and 66.7% was silt & clay.

3.1.2 Atterberg's Limit Test Results

Theses test was conducted only for sample no. 1 and 2, as sample no. 3 could not passed through the sieve # 200.

The plastic limit test was conducted for sample no. 1and sample no. 2. The threads were made on the flat non porous surface and the thickness of the threads was measures. The plastic limit for sample no. 1 was 16.4% and for sample no. 2 it was 16.3%. With these plastic limits the samples was shows the low plastic limit.

The liquid limit test was conducted for sample no. 1 and 2. A graph was plotted between numbers of blows verses percentage water content. The liquid limit of sample no. 1 was evaluated as 21.5%. The sample no. 2 was evaluated 21.2%.

From the soil samples it was observed that minimum liquid limit value was 21.2 and it exceed maximum to 21.5. The averaged value of liquid limit was 21.4 and standard deviation was only 0.2. Plastic limit ranges from 16.3 to 16.4. The average value was 16.4 and standard deviation from mean value was 0.1.

3.1.3 Plastic Index

The plastic index was calculated using the flowing equation number 5.

$$P.I = L.L - P.L \quad \ldots\ldots (5)$$

Sample no.1:

P.I = 21.5 – 16.4
P.I = 5.1

Sample no. 2:

P.I = 21.2 – 16.3
P.I = 4.9

Table 3.1. Summary of Atterberg's limit tests and sieve analysis results.

Sr. No.	Sample No.	Grain Size Analysis % Passing sieve # 200			Atterberg' s Limits			NMC	Degree of Saturation %	Porosity %	Unified Classification
		Gravel (%)	Sand (%)	Silt/Clay (%)	L.L	P.L	P.I				
1	1	0	2	98	21.5	16.4	5.1	12.7	7.1	71.3	CL
2	2	0	3	97	21.2	16.3	4.9	1.8	7.3	71.2	CL
3	3	38	57	5	NP	NP	NP	2.1	-	-	GM
Average		12.7	20.7	66.7	21.4	16.4	5.0	5.5	7.2	71.3	CL
Standard Deviation		21.9	31.5	53.4	0.2	0.1	0.1	6.2	0.1	0.1	

According to the P.I values: 0 – Nonplastic; (1-5)- Slightly plastic; (5-10) - Low plasticity; (10-20)- Medium plasticity; (20-40)- High plasticity; and >40 Very high plasticity.

According to these classes the sample no. 1 was slightly plastic and sample no. 2 was low plastic. The P.I value ranges from 4.9 to 5.1 and average was 5.0. It was evaluated from the results that landslide debris has maximum content of clay with low plasticity. It was also observed that debris material has cementation minerals, which on getting wet the cohesion force increases and erosion reduces to great degree. Due to this phenomenon the large boulders are present in the debris material. The swelling phenomenon was also observed in the material which is the cause of large clay content. On getting wet the soil (clay) swells and cohesion force increase within the material due to the presence of cementation minerals, hence, the erosion of debris material reduces. Vise versa on getting dry the clay shrinks. The clay swelling and cohesion force phenomenon are the reason due which the dam was not breached yet, as very small erosion was observed. The two seepage points was also observed in the debris material on the landslide location.

3.2 HEC-RAS Results

In HEC-RAS the unsteady flow simulation editor was used to simulate the flood inundation in result of Attaabad Lake breach. The flow hydrograph for upstream boundary condition, normal depth for downstream boundary condition and inline structure parameters as an input to breach were added (table 3.2 and figure 3.1). The unsteady model was then run to simulate for x-y-z perspective plot of flood extend, stage and flow hydrograph, velocities, volume, stream power and hydraulic depth in the form of graphs.

Table 3.2. Inline structure breach parameters.

Bottom width	190 m
Bottom elevation	2329.73 m
Right side slopes	1
Left side slopes	1
Breach weir coefficient	2.6
Full Formation Time (hrs)	3
Starting WS	2400 m
Center station	1950 m
Failure Mode	Overtopping

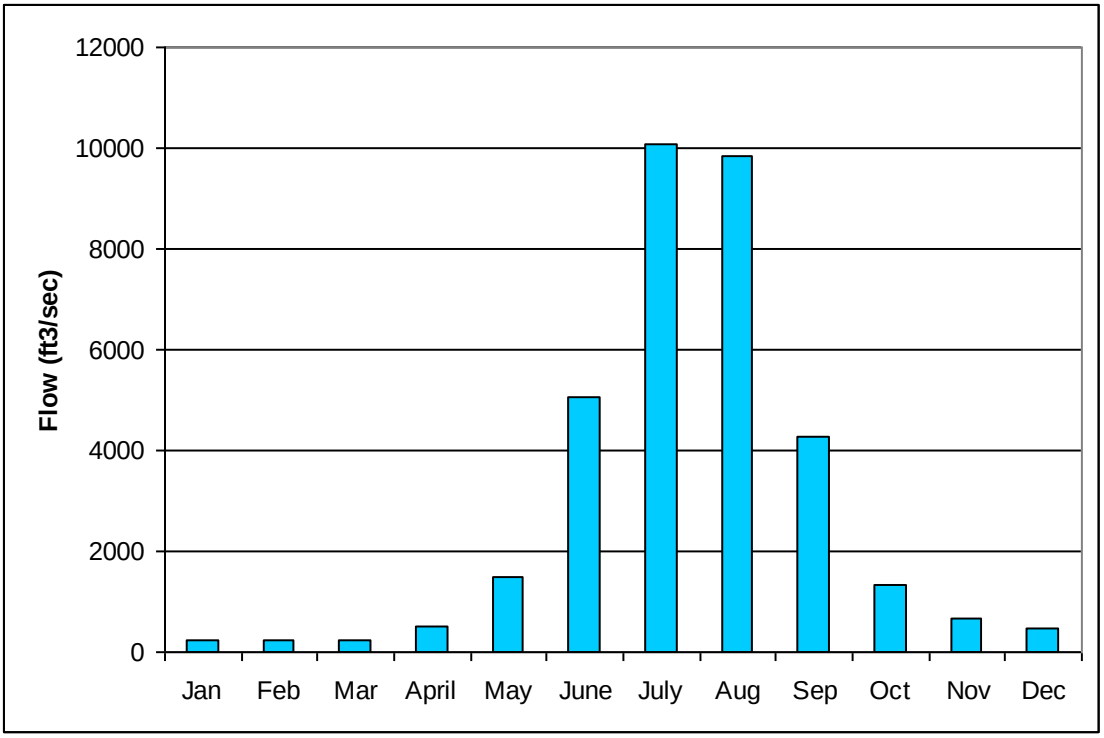

Figure 3. 1. Estimated monthly average flows at landslide location.

3.2.1 X-Y-Z Perspective Plot

The x-y-z perspective plot gives the view of flood extent in 3D along with cross sections and station numbers in HEC-RAS model (figure 3.2).

3.2.2 Flow Hydrograph

The flow hydrograph shows the flood discharge (Q in m^3/sec) along the Hunza River. It shows the flow in the main channel, left overbank and right overbank in the river. The flow hydrograph (figure 3.3). It was observed that the flow is very high in the main channel that is the center of the river as compared to left and right bank flow. The highest flow value 940,000 m^3/sec in the main channel was observed at distance of 30 km from landslide location.

3.2.3 Velocity Graph

The velocity graph shows the flood wave velocity throughout along the Hunza River (figure 3.4). The graph shows that the flood wave velocities were very high in the main channel as compared to left and right river bank. The maximum velocity was reached to about 34 m/sec at distance of 70 km from the landslide location. The velocity was also very high at the beginning of the simulation.

3.2.4 Volume Graph

The volume graph shows the volume of flood water at various points throughout the Hunza River. The volume was very high at the beginning of the simulation it gradually lowers while moving downstream (figure 3.5).

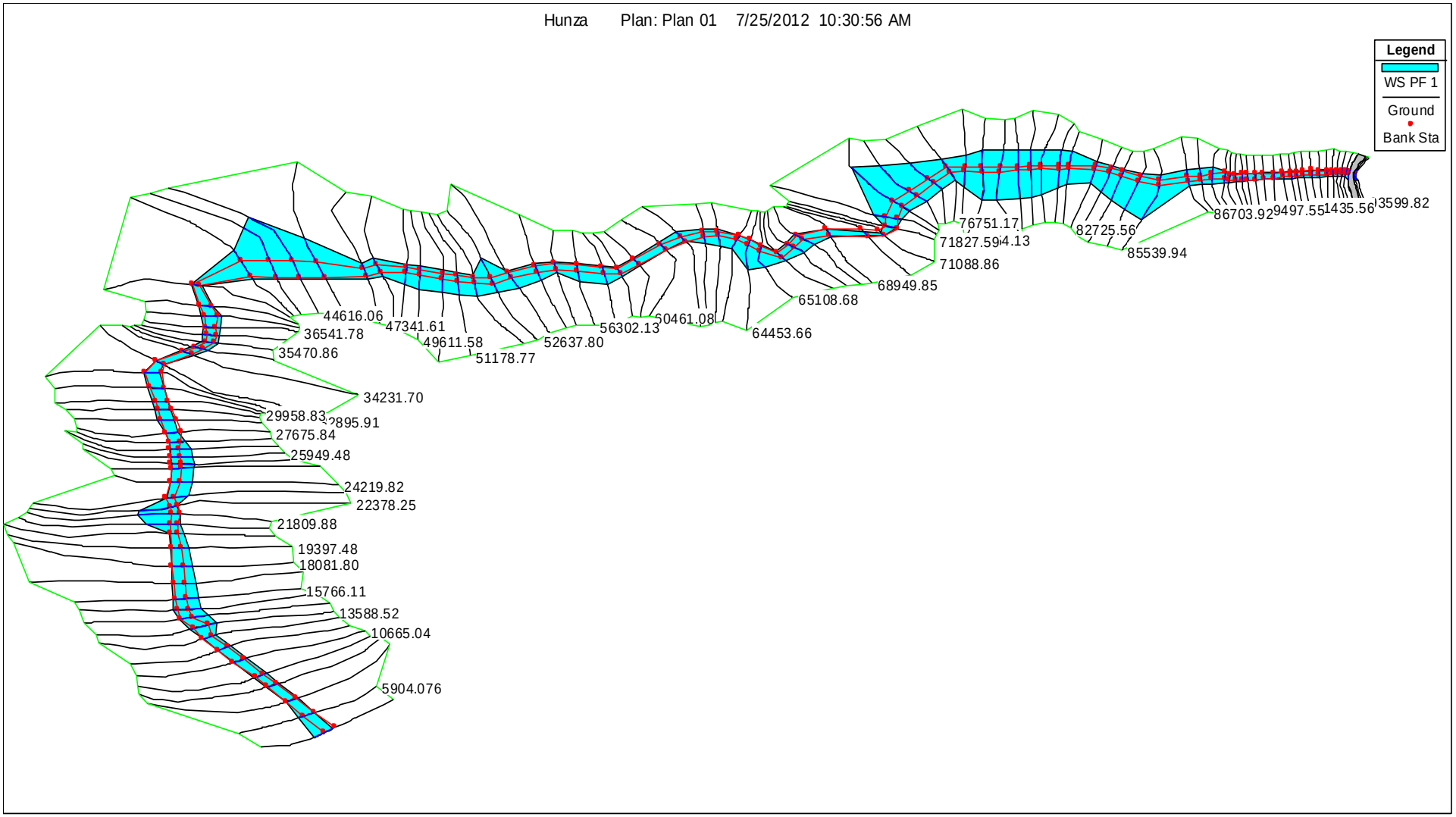

Figure 3. 2. X-Y-Z perspective plot of flood extent in HEC-RAS.

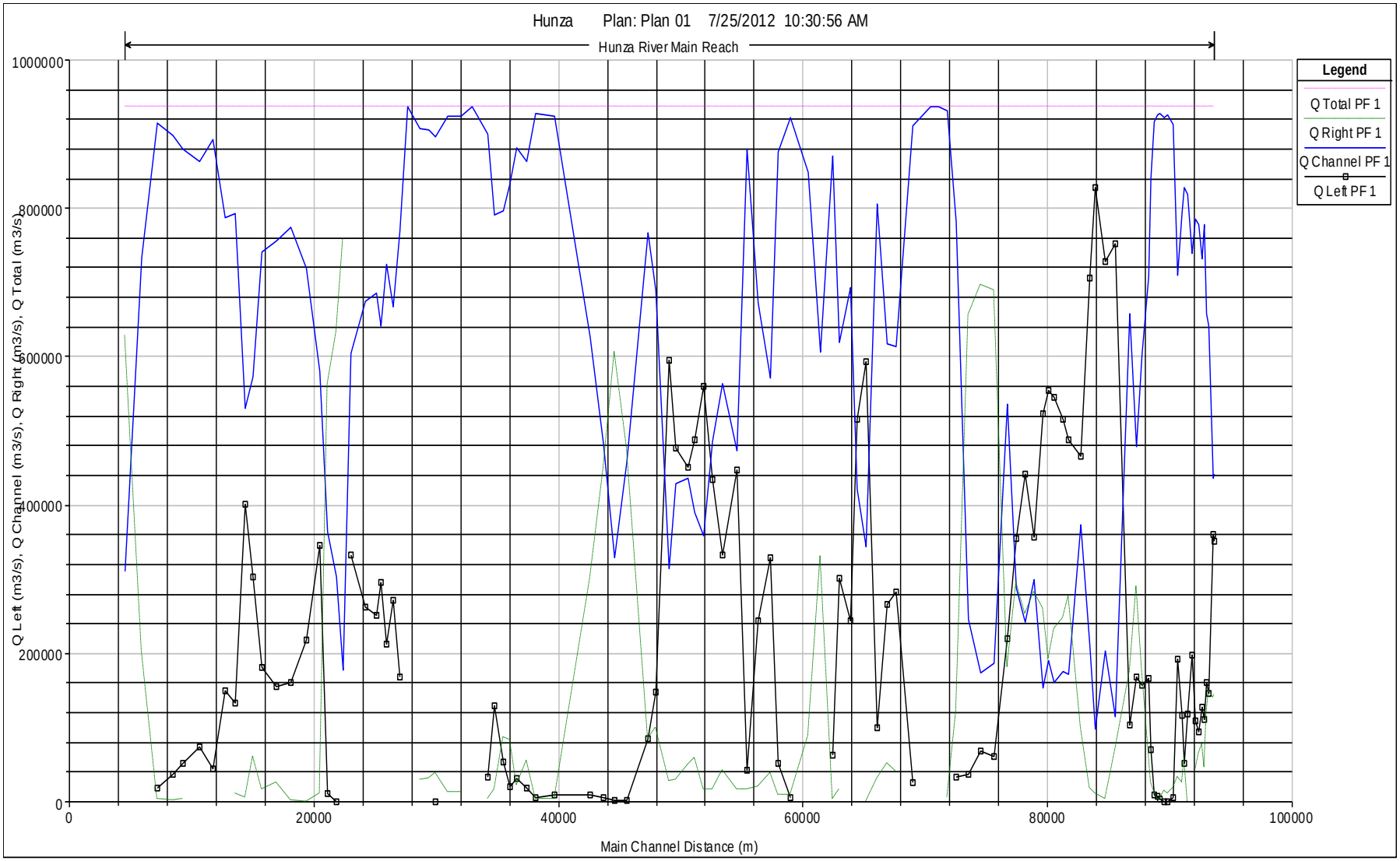

Figure 3. 3. Flow hydrograph showing the flow in main, left and right channel.

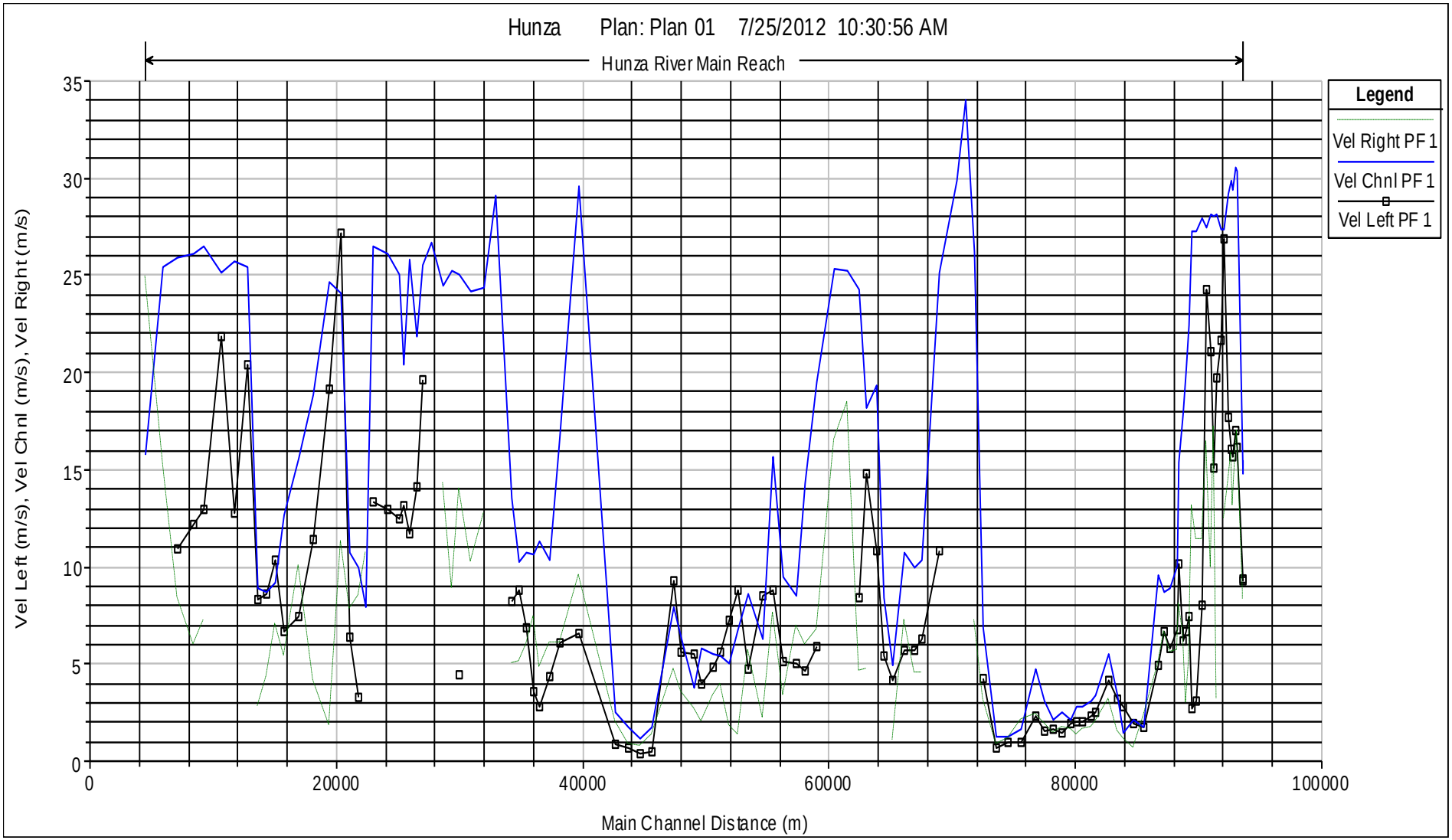

Figure 3. 4. Graph showing the flood wave velocity in main channel, left and right overbank.

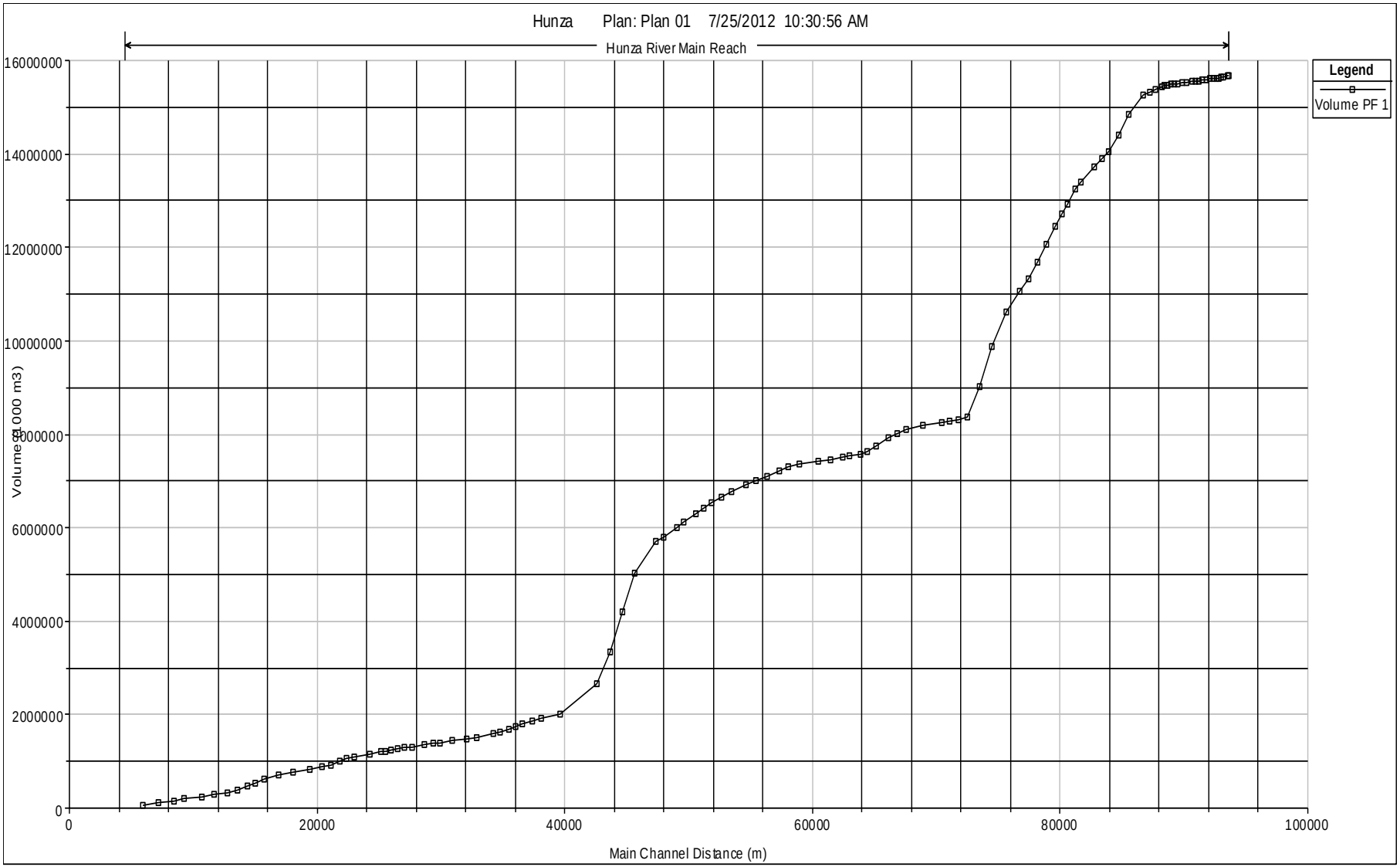

Figure 3. 5. Graph showing the water volume along the Hunza River.

3.2.5 Stream Power Graph

The stream power graph shows the flood wave power in the main channel, left overbank and right overbank. The maximum stream power was observed in the main channel, while power was negligible at left and right overbank while compared to the main channel (figure 3.6).

3.2.6 Hydraulic Depth Graph

The hydraulic depth shows the depth of flood water as calculated from one cross section to the next throughout the Hunza River. The depth was high in the main channel as obvious because it is from the river bed. The maximum depth was observed at distance of almost 70 km from Attaabad (figure 3.7).

3.3 Flood Extent Analysis

The HEC-RAS results were imported in GIS format using the HEC-GeoRAS. The flood extent map was prepared in the ArcGIS. The villages which lie in the flood extent were identified. It was observed that 26 villages along the Hunza River bank were potentially at risk being inundated by the flood. The villages closer to the river banks were at high risk. The flood extent map showing the villages at risk (figure 3.8).

3.4 Flood Water Depth Analysis

The flood water depth map was prepared in ArcGIS. The water depth was divided in six classes with the interval of 50 m. The water depth was low up to Ahmad Abad village about 150 m from the river bed which is at high elevation. The flood extent was also small due to narrow river corridor and steep slopes along the river bank. After the village Ahmad Abad the river width becomes wider and river bed reduced in elevation. Here the

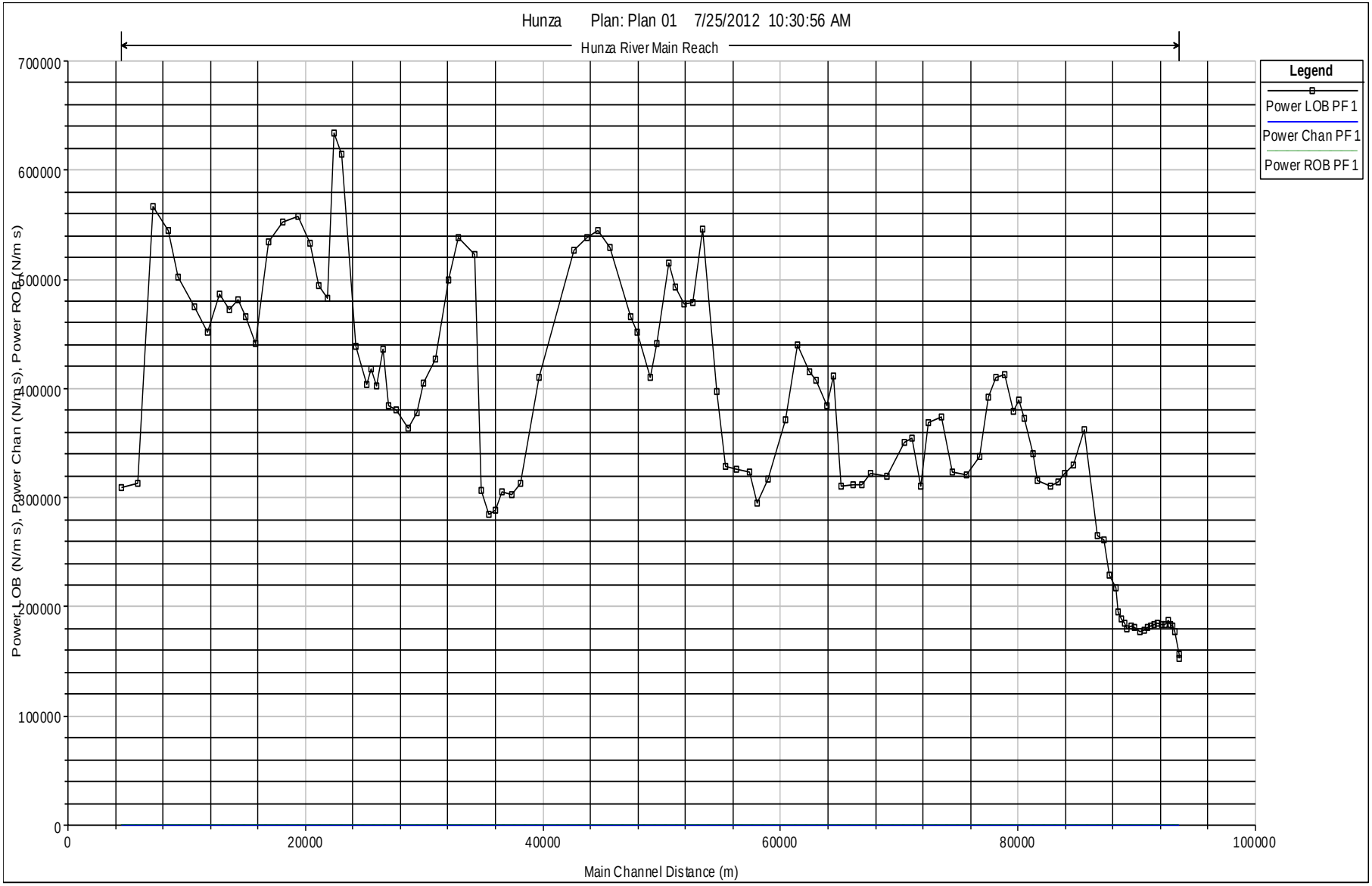

Figure 3. 6. Graph showing the stream power in the main channel.

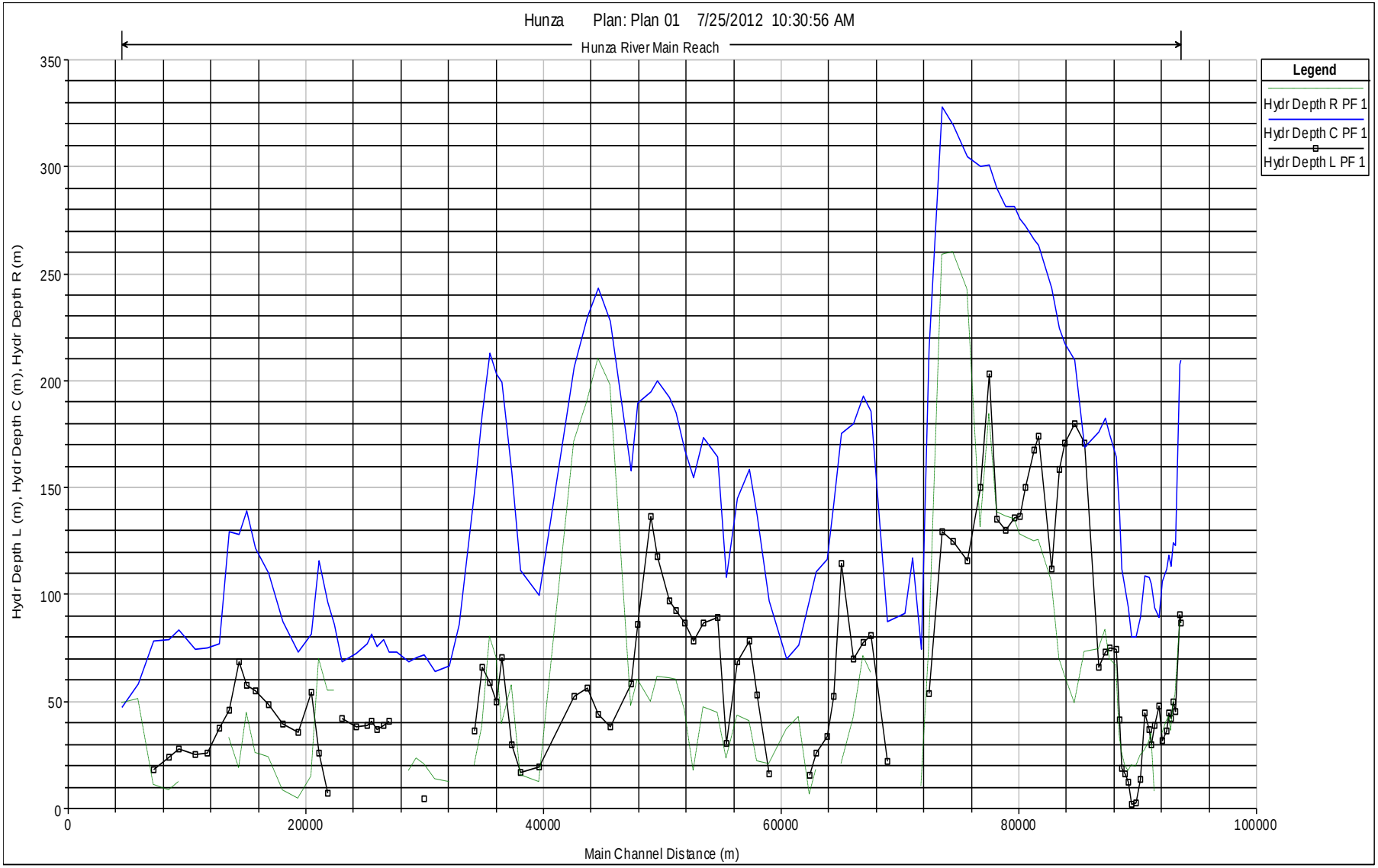

Figure 3. 7. Graph showing the hydraulic depth in main channel, left and right overbank.

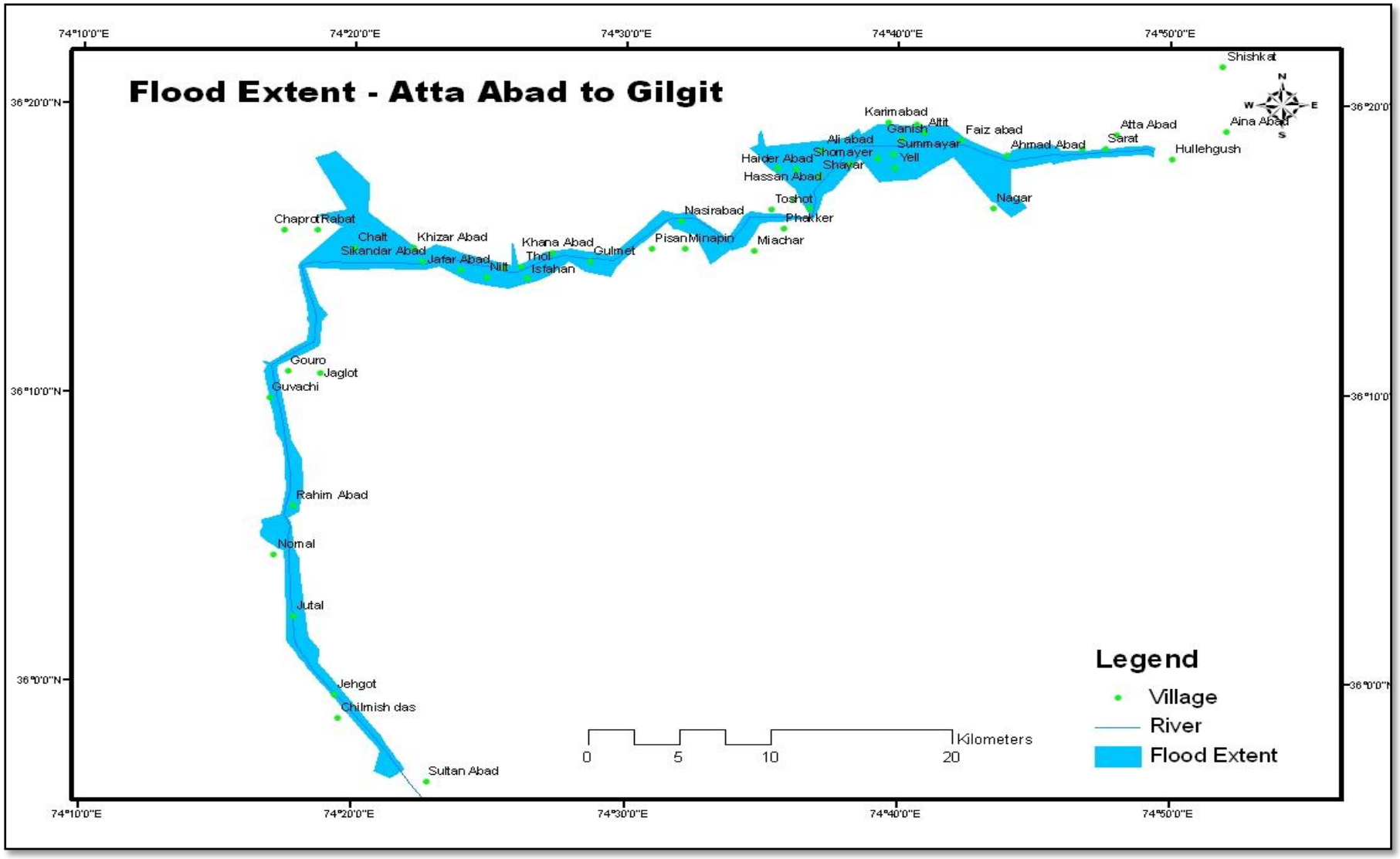

Figure 3. 8. Map showing the flood extent along the Hunza River.

maximum flood depth was observed about > 250m starting from Faiz Abad village to Toshot village. The model predicted the extent of flood to be wider in this area. Moving downstream up to Jaffar Abad village the model predicted reduced flood extent and flood water depth in this part of the valley. The predicted water depth was observed between 0 – 100 m and 100 – 200 m. In the next part of observation the flood depth and extent again become high but not as high as it was observed in second part. The depth and extent were high between Khizar Abad and Sikander Abad village. After this the flood extent and depth was small until it reach the Gilgit village (figure 3.9). The inundated villages were also classified as at high risk, medium risk and low risk. The 7 villages were at high risks which were Ganish, Summayar, Shayar, Ali Abad, Haider Abad, Chalt and Sikander Abad. The 10 villages are at medium risk which was Faiz Abad, Altit, Yell, Shomayar, Hassan Abad, Gulmet, Thol, Maiun, Jaffar Abad and Jutal. The 9 villages were at low risk which was Askur Das, Hakuchar, Nasirabad, Khana Abad, Isfahan, Nilt, Khizar Abad, Rahim Abad and Jehgot. The detail water depth for all the 26 villages at risk is given in table 3.2.

3.5 Flood Velocity Analysis

The flood velocity map was also prepared in the ArcGIS using the HEC-GeoRAS. The velocity points were marked in the flood extent from Attaabad to Gilgit. It was analyzed that the flood wave velocity was very high at the beginning then it become gradually low downstream. While moving downstream towards Gilgit it becomes again high. The model predicted that the velocity was very high initially due to high water discharge and narrow river gorge at this location of the valley. The velocities were low with large flood extent and high water depth. The flood velocity was high where the water depth was low and flood extent was also less wide (figure 3.10 & table 3.2).

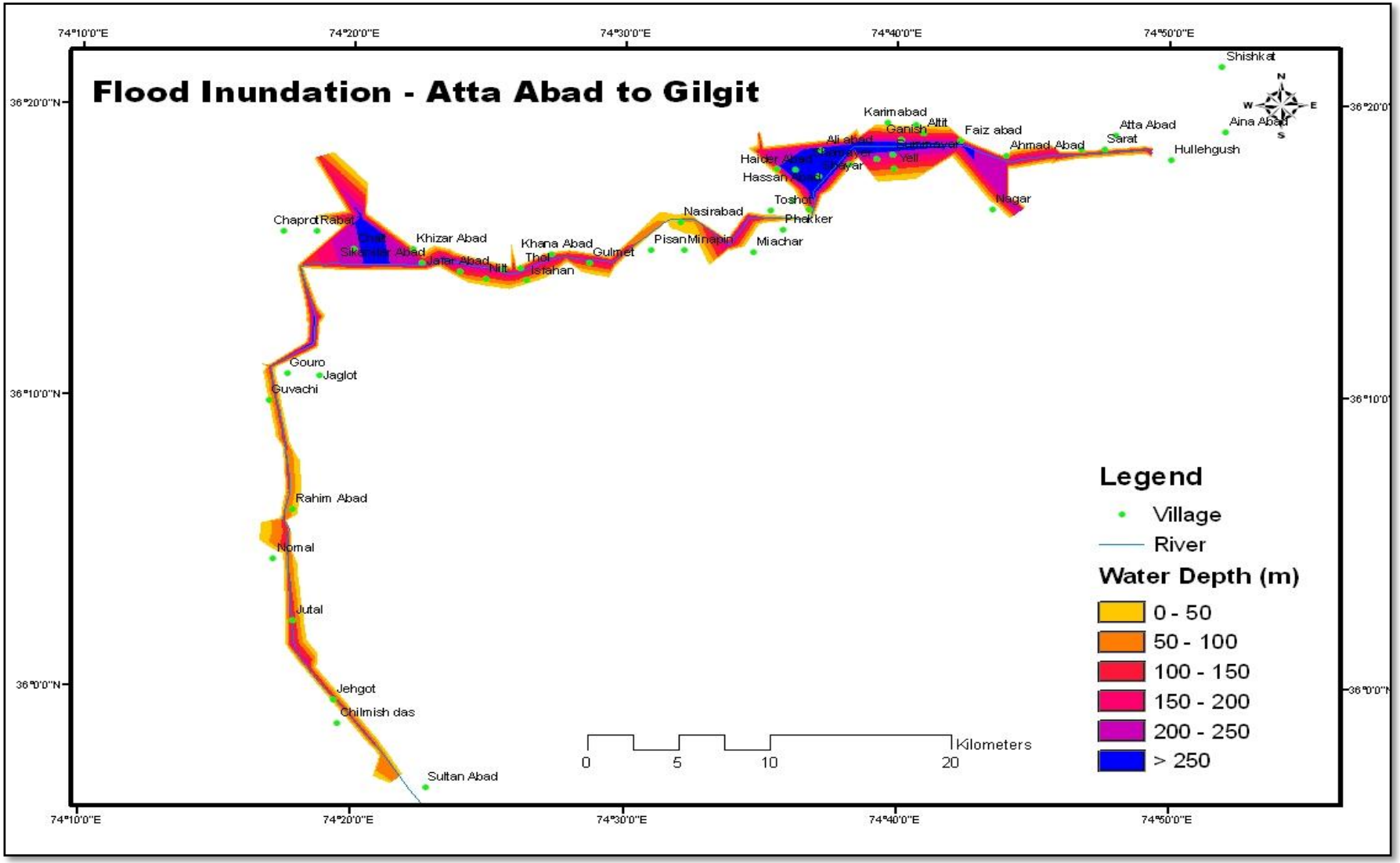

Figure 3. 9. Map showing the flood water depth along Hunza River.

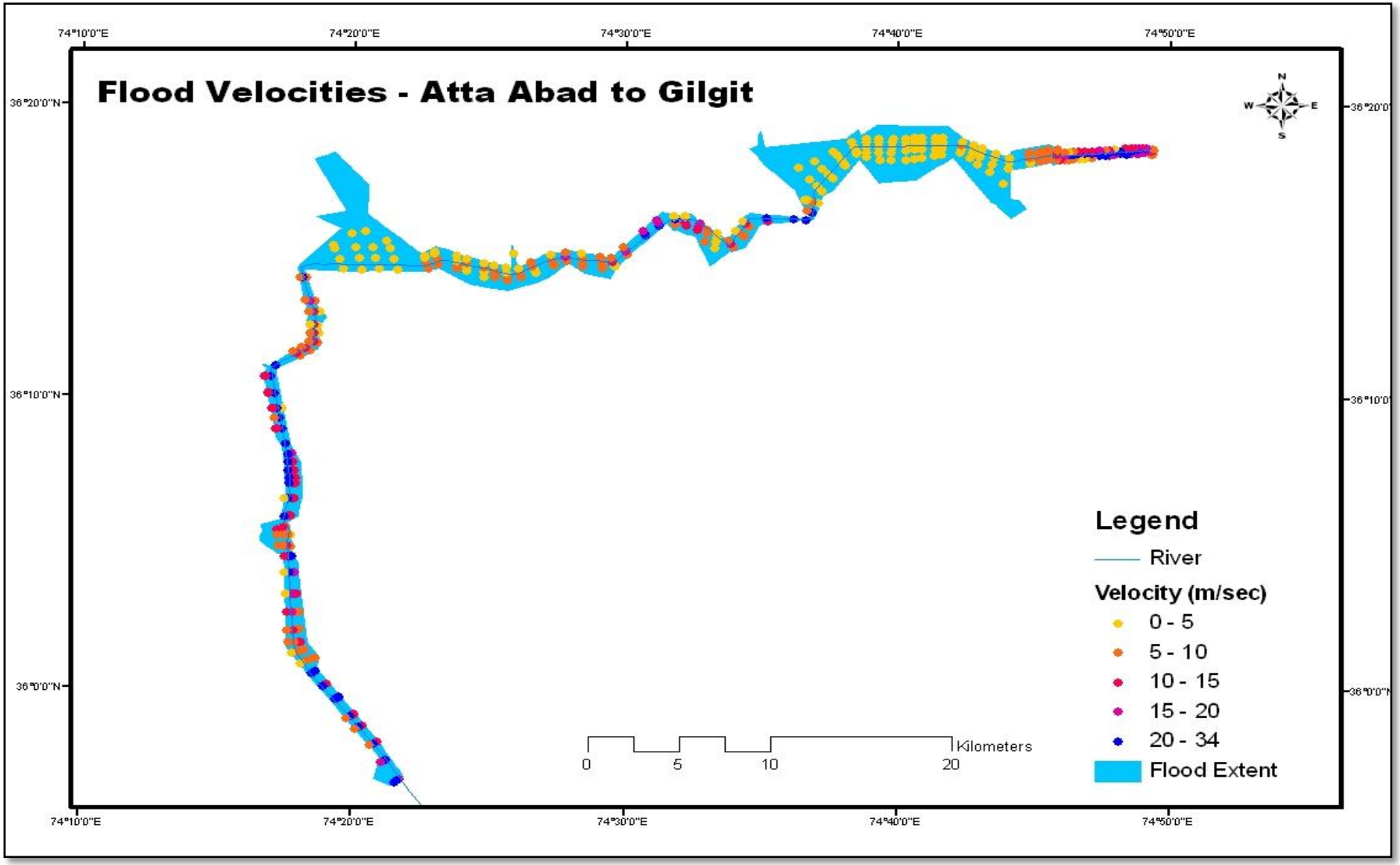

Figure 3. 10. Map showing the flood wave velocity along the Hunza River in the maximum flood extent area.

Table 3. 3: Water Depth, velocity and time to reach maximum discharge for inundated villages.

Village Name	Water Depth (m)	Velocity (m/s)	Time of Maximum Discharge
Faizabad	160	4.3	50 min
Altit	110	2	1 hr
Ganish	215	2.54	1 hr 10 min
Summayar	225	2.54	1 hr 10 min
Yell	100	1.8	1 hr 10 min
Shomayar	200	2.54	1 hr 10 min
Akur Das	50	1.8	1 hr 20 min
Ali Abad	280	2	1 hr 20 min
Shayar	310	2.54	1 hr 25 min
Hassan Abad	155	1.5	1 hr 35 min
Haider Abad	300	2.54	1 hr 30 min
Hakuchar	75	11.3	1 hr 50 min
Nasirabad	70	8.79	2 hr 5 min
Gulmet	140	4.6	2 hr 15 min
Khana Abad	50	7.9	2 hr 20 min
Thol	125	3.6	2 hr 20 min
Isfahan	51	5.62	2 hr 20 min
Maiun	150	3.4	2 hr 25 min
Nilt	80	2.54	2 hr 25 min
Jaffarabad	135	2.2	2 hr 25 min
Sikandar Abad	210	7.3	2 hr 30 min
Khizar Abad	45	2.6	2 hr 30 min
Chalt	235	2.54	2 hr 35 min
Rahimabad	40	10.7	4 hr
Jutal	190	15.57	4 hr 10 min
Jehgot	70	30	4 hr 20 min

Chapter 4

CONCLUSIONS AND RECOMMENDATIONS

4.1 Conclusions

Following conclusions could be drawn based on the field visit and hydrological simulation modeling in GIS of the Landslide Lake.

1. The information collected from the local community and lake monitoring authority it was concluded that the landslide occurred at the fault line. The crack was first observed in February, 2003 and the noise from the crack was heard by the local residents from many years. The landslide created highly crushed rock mass. The debris materials consist of large boulders, cobbles, silt and plastic clay. The percentage of silt and clay varies in debris material. The landslide lake height is 126 m above the river bed, width 250 to 350 m and length along the river is 23 km. The landslide lake created a potential storage of 305 MCM, but with 30 m cut it was reduced to 133 MCM (56% reduction).
2. Hydrologic Engineering Center's River Analysis System (HEC - RAS) was used for the potential inundation modeling. The unsteady flow simulation in HEC-RAS proves to be very useful for forecasting of flood inundation areas. The peak discharge was observed to take 10 hr 20 min to reach the Gilgit River. In total 26 villages could be inundated in case of dam breach. Seven villages were categorized as at high risk including Ganish, Summayar, Shayar, Ali Abad, Haider Abad, Chalt & Sikander Abad. While 10 villages were catagorized as at medium risk including Faiz Abad, Altit, Yell, Shomayar, Hassan Abad, Gulmet, Thol, Maiun, Jaffar Abad & Jutal. However, nine

villages categorized at low risk including Askur Das, Hakuchar, Nasirabad, Khana Abad, Isfahan, Nilt, Khizar Abad, Rahim Abad & Jehgot.

4.2 Recommendations

In light of the study the following recommendation could be drawn:

1. An emergency preparedness plan should be prepared on the basis of dam break studies results. The main effect of the dam break will be flood inundation and high velocity flood wave.
2. The secondary effect will be the landslide in the lake area due to saturation and rapid drawdown and along the river due to river bank erosion.
3. People living downstream & lower elevation and on terrace edges (unstable slopes) are at high risk. These people should be moved to high elevated and stable areas.
4. Emergency plan should be prepared while considering that bridges and roads could be highly damaged.
5. All the communities living in the vulnerable areas should be trained to cope with the disaster.
6. A study should be taken to analyze the impact of flood inundation on Terbela Dam.

REFERENCE

Brunner, G. W. (January, 2010). HEC-RAS River Analysis System User's Manual. Version 4.1. US Army Corps of Engineers Hydrologic Engineering Center (HEC).

Eisbacher , G. H. , and Clague , J . (1984). Destructive mass movements in high mountains - hazard and management, Geol, Sur. Canada Paper 84- 16.

Gasiev, E. (1984). Study of the Usoy landslide in Pamir. Proceedings, 4th International Symposium on Landslides: v. 1, Canadian Geotechnical Society, Toronto, p. 511 - 515.

Geotechnical Engineering Bureau (April, 2007). Test Method for Liquid Limit, Plastic Limit and Plasticity Index. Geotechnical Test Method (GMT) 7. Revision#1. New York State Department of Transportation. Retrieved from https://www.dot.ny.gov/divisions/engineering/technical-services/technical-services-repository/GTM-7b.pdf

GREE. Unified Soil Classification System. GREE Drilling and Testing, INC. and GREE in situ, INC. Environmental and Geotechnical Testing Services.

Gupta Vikram & M. P. Sah (19 September 2007). Impact of the Trans-Himalayan Landslide Lake Outburst Flood (LLOF) in the Satluj catchment, Himachal Pradesh, India Natural Hazards. Volume 45, Number 3, 379-390

Holmes, Arthur (1965). Principles of physical geology. Edition 2nd. New York, Ronald Press Co. 1288 p.

Krishna Reddy. Experiment 6 Grain Size Analysis (Sieve and Hydrometer Analysis). Engineering Properties of Soils Based on Laboratory Testing. UIC p.61. Retrieved from http://www.uic.edu/classes/cemm/cemmlab/Experiment%206-Grain%20Size%20Analysis.pdf

Krishna Reddy. Experiment 7 Atterberg Limits. Engineering Properties of Soils Based on Laboratory Testing. UIC p.61. Retrieved from http://www.uic.edu/ classes/ cemm /cemmlab/Experiment%207-Atterberg%20Limits.pdf

Li, Ming-Hsu, Ming-Hsi Hsu, Lung-Sheng Hsieh and Wei-Hsien Teng (2002). Inundation Potentials Analysis for Tsao-Ling Landslide Lake Formed by Chi-Chi Earthquake in Taiwan. Natural Hazards 25: 289–303, 2002.

Lillesand T. M. & Kiefer R. W., (2000). Remote Sensing and Image Interpretation. 4th edition. Wiley & Sons.

Merwade, Venkatesh. (November, 2009). Tutorial on using HEC-GeoRAS with ArcGIS 9.3. School of Civil Engineering Purdue University.

Mir, Shabir Ahmed (May 17, 2010). Spillway in Attabad Lake completes to ease pressure. Retrieved from http://tribune.com.pk/story/13714/spillway-in-attabadlake-complete-to-ease-pressure/

ODOT (2010). Appendix A Hydraulic Roughness (Manning n) Values of Conduits and Channels. Oregon Department of Transportation. Retrieved from ftp://ftp.odot.state.or.us/techserv/Geo-Environmental/Hydraulics/Hydraulics%20Manual/Chapter_08/CHAPTER_08.pdf

Peng Cui, Ying-yan Zhu, Yong-shun Han, Xiao-qing Chen and Jian-qi Zhuang (June 30, 2009). The 12 May Wenchuan earthquake-induced landslide lakes: distribution and preliminary risk evaluation. Landslides. 6:209–223. Springer-Verlag 2009.

Richard Hughes (February, 2010). Attaabad Landslide - Hunza Valley, Northern Areas Pakistan. Consultant Aga Khan Cultural Services, EEFIT.

Schuster RL (2000). A worldwide perspective on landslide dams. In: Usoi landslide dam and lake Sarez—an assessment of hazard and risk in the Pamir mountains, Tajikistan. UN, ISDR Prevention Series 1:19–22

UTA (February, 2004). Atterberg Limit Test (Lecture Notes 5). University of Texas at Arkington. Retrieved from http://www.uta.edu/ce/geotech/lab/Main/Soil%20Lab/05_atterberg%20Limit%20tests/atterberg%20limit%20test.pdf

Wikipedia (2010). Causes of Landslides. Retrieved from http://www.answers.com/topic/causes-of-landslides#Water-level_change

Wikipedia (29 April, 2012). Sieve Analysis. Retrieved from http://en.wikipedia.org/wiki/Sieve_analysis#cite_note-0

Wikipedia (16 June, 2012). Atterberg Limits. Retrieved from http://en.wikipedia.org/wiki/Atterberg_limits.

Xue-Cai F. and An-ning G. (1986). Principle Characteristics of Earthquake Landslides in China. Geologia Applicata e Idreogeologia (Italy) 21(2): 27-45.

APPENDICIES

Appendix-1. LANDSAT-7 ETM+ Mosaic Image of the study area taken from U.S. Geological Survey, Earth Resources Observation & Science Center (EROS) website.

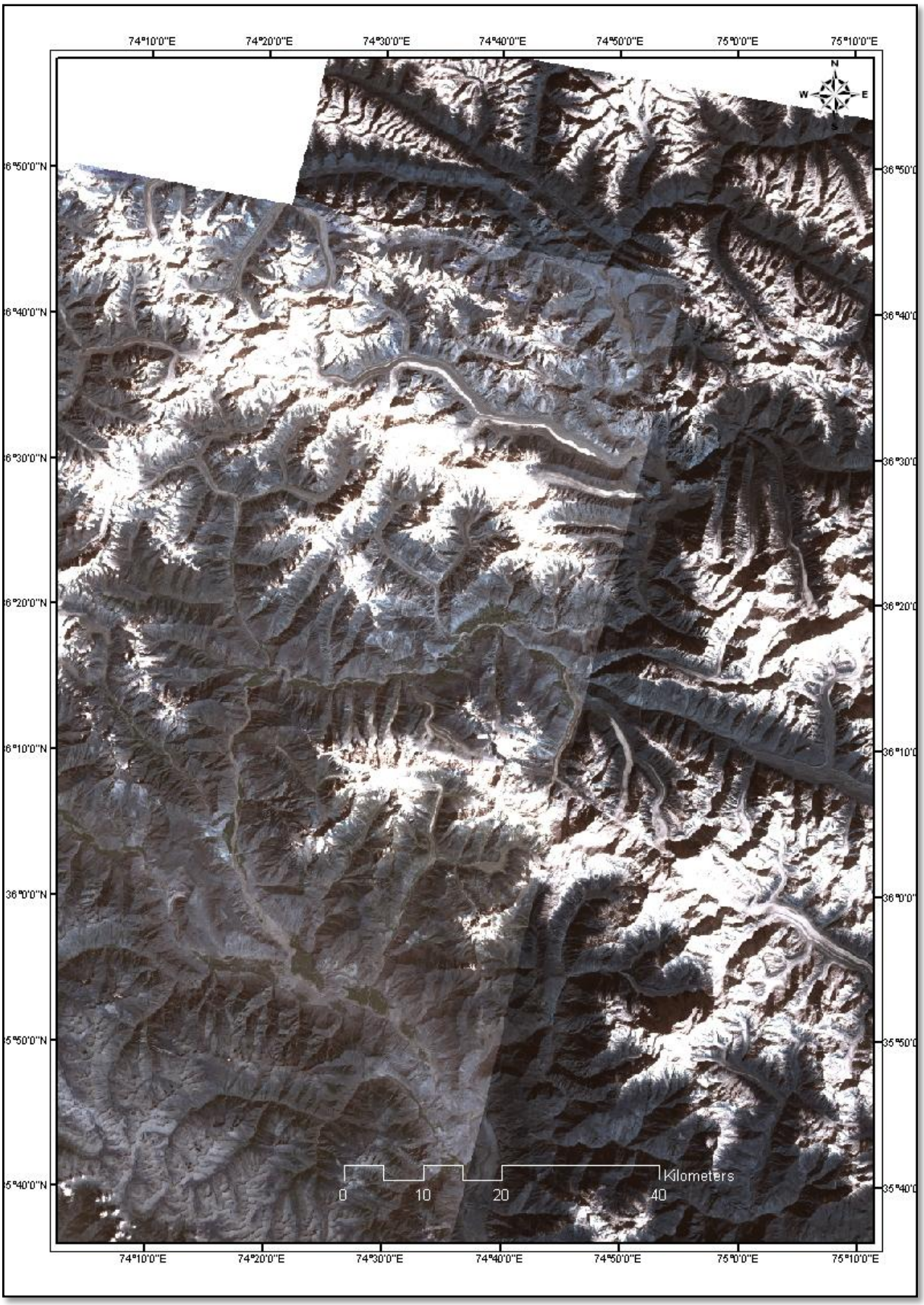

Appendix-2. Digital Elevation Model (DEM) of 30m produced by Shuttle Radar Topography Mission (SRTM) and downloaded from United States Geological Survey (USGS) website.

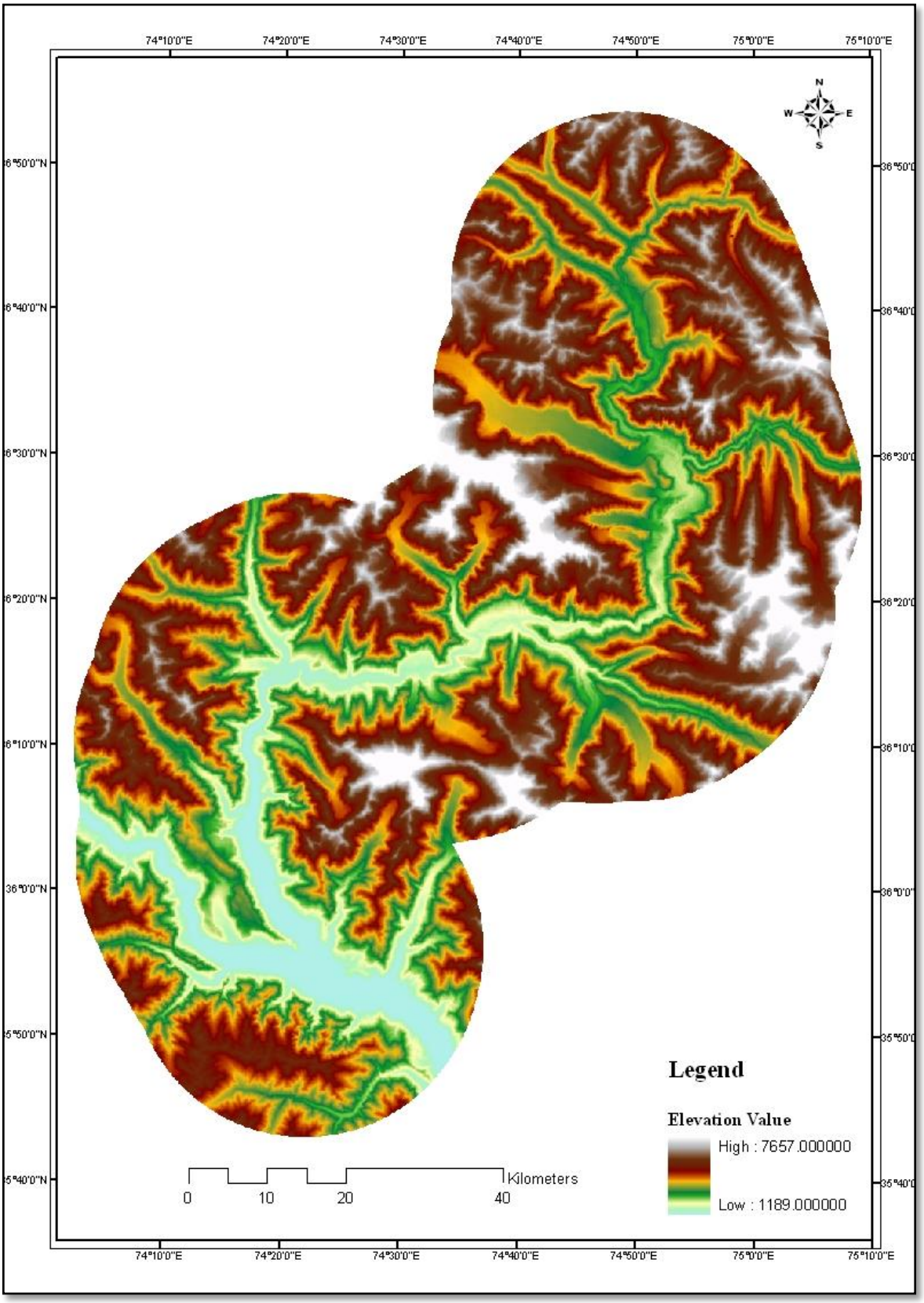

Appendix-3. Observed monthly average flows at Daniyor Bridge. Data collected from Water and Power Development Authority (WAPDA), Lahore, Pakistan.